SUPPORTING INFORMATION

$CaSc_2O_4$ Hosted Upconversion and Downshifting Luminescence

Tian Wei, [a#] Yingdong Han, [d#] Yang Wei, [a] Chao Gao, [c] Hui Ma, *[a] Fan Zhang, [a] Shuyi Bao, [a] Su Jing, *[b] Ling Huang, *[a]

[a]Institute of Advanced Materials, Jiangsu National Synergetic Innovation Center for Advanced Materials, Nanjing Tech University, Nanjing 211816, China

[b]School of Chemistry and Molecular Engineering, Nanjing Tech University, Nanjing 211816, China

[c]School of Inspection and Testing Certification, Changzhou Vocational Institute of Engineering, Changzhou 213164, China

[d]School of Precision Instruments and Optoelectronics Engineering, Tianjin University, Tianjin 300072, China

[#] These authors contributed equally.

Table S1 Typical Sc-based luminescent materials.

No.	Host material	Preparation method	Emission color	Size, morphology	Reference
1	Na_xScF_{3+x}:Yb/Tm/Er (18/0.2/x mol %)	Thermal coprecipitation	Green, red	27-36 nm nanoparticles	*J. Am. Chem. Soc.*, 2012, **134**, 8340-8343.
2	KSc_2F_7:Yb/Er	Thermal coprecipitation	red	376 nm nanorods	*Nanoscale*, 2013, **5**, 11928-11932
3	$ScPO_4 \cdot 2H_2O$:Ce,Tb	Hydrothermal	Green	2 μm micro-spheres	*J. Mater. Chem. C*, 2015, **3**, 12385-12389
4	Na_xScF_{3+x}:Yb/Er	Thermal coprecipitation	From orange-red to green.	~ 100 nm nanospheres and nanocubes	*Nanoscale***,** 2015, **7**, 4048-4054
5	ScOOH:Eu, ScOOH:Tb	Hydrothermal	Red, green	1 μm microcrystals	*Adv. Mater.*, 2016, **26**, 6665-6671.
6	KSc_2F_7:Yb/Er	Thermal coprecipitation	Red	100 nm nanorods	*J. Mater. Chem. C*, 2017, **5**, 3503−3508
7	$ScVO_4$:Eu/Dy/Sm	Hydrothermal	Red, green, blue	10 μm microcrystals	*J. Rare Earth.*, 2017, **35**, 28-33.
8	KSc_2F_7:Yb/Er, K_2NaScF_6:Yb/Er	Thermal coprecipitation	Red	~ 168.3 nm nanorods	*Dalton Trans.*, 2018, **47**, 4950-4958
9	Sc_2O_3:Eu^{2+}/Eu^{3+}	Thermal decomposition	Red, purple	≈ 20 nm nanoparticles	*Adv. Mater.*, 2018, **30**, 1705256.
10	ScF_3: Yb/Er, $ScF_{2.6}$: Yb/Er	Thermal coprecipitation	Green, yellow, blue	≈ 100 nm nanoparticles	*Chem. Mater***,** 2017, **29**, 9758-9766.

Table S2 Rietveld refinement of the crystallographic and structural parameters of $CaSc_2O_4$ and $CaSc_2O_4$:Yb/Tb (5/0.1 mol%).

Compounds	$CaSc_2O_4$	$CaSc_2O_4$:Yb/Tb (5/0.1 mol%)
Crystal system	orthorhombic	orthorhombic
Lattice parameters	Pnam	Pnam
$\alpha = \beta = \gamma = 90°$	a = 9.4555	a = 9.4747
(Å)	b = 11.1073	b = 11.1461
	c = 3.1404	c = 3.1537
V (Å)	V = 329.8211	V = 333.0457
Rwp(%)	9.7690	8.8500
Rp(%)	7.4100	6.7810
R_{exp}	9.0100	6.6500
χ^2	1.0830	1.3310

Table S3 Structural parameters and refinement data of $CaSc_2O_4$ and $CaSc_2O_4$:Yb/Tb (5/0.1 mol%).

Atom		$CaSc_2O_4$	$CaSc_2O_4$: Yb/Tb (5/0.1 mol%)
Ca1	x	0.7536	0.7528
	y	0.6537	0.6552
	z	0.2500	0.2500
Sc1	x	0.4198	0.4247
	y	0.1071	0.1084
	z	0.2500	0.2500
Yb1	x	0.0000	0.4247
	y		0.1084
	z		0.2500
Tb1	x	00.0000	0.4247
	y		0.1084
	z		0.2500
Sc2	x	0.4279	0.4202
	y	0.6125	0.6132
	z	0.2500	0.2500
Yb2	x	0.0000	0.4202
	y		0.6132
	z		0.2500

Table S3 Structural parameters and refinement data of $CaSc_2O_4$ and $CaSc_2O_4$:Yb/Tb (5/0.1 mol%). (Continued)

Tb2	x	0.0000	0.4202
	y		0.6132
	z		0.2500
O1	x	0.2045	0.1948
	y	0.1699	0.1670
	z	0.2500	0.2500
O2	x	0.1287	0.1252
	y	0.4752	0.4788
	z	0.2500	0.2500
O3	x	0.5233	0.5168
	y	0.7811	0.7891
	z	0.2500	0.2500
O4	x	0.4199	0.4100
	y	0.4233	0.4219
	z	0.2500	0.2500

Table S3 Structural parameters and refinement data of $CaSc_2O_4$ and $CaSc_2O_4$:Yb/Tb (5/0.1 mol%). (Continued)

Bond lengths (Å)		
Sc1-O1	2.1520	2.2740
Sc1-O2	2.1760	2.1320
Sc1-O3	2.0730	2.1900
Sc2-O4	2.1670	2.1370
Sc1-Sc1	3.1404	3.1537
Sc2-Sc2	3.1404	3.1537
Yb1-Tb1		3.1537
Yb2-Tb2		3.1537
Bond angles (o)		
O2-Sc1-O2	91.2800	92.1300
O3-Sc1-O3	98.5100	102.3300
Sc1-O2-Sc1	91.2800	96.2300
Sc2-O1-Sc2	96.3700	103.410
Yb1-O2-Tb1		96.2300
Yb1-O3-Tb1		102.3300
Yb2-O4-Tb2		97.4900

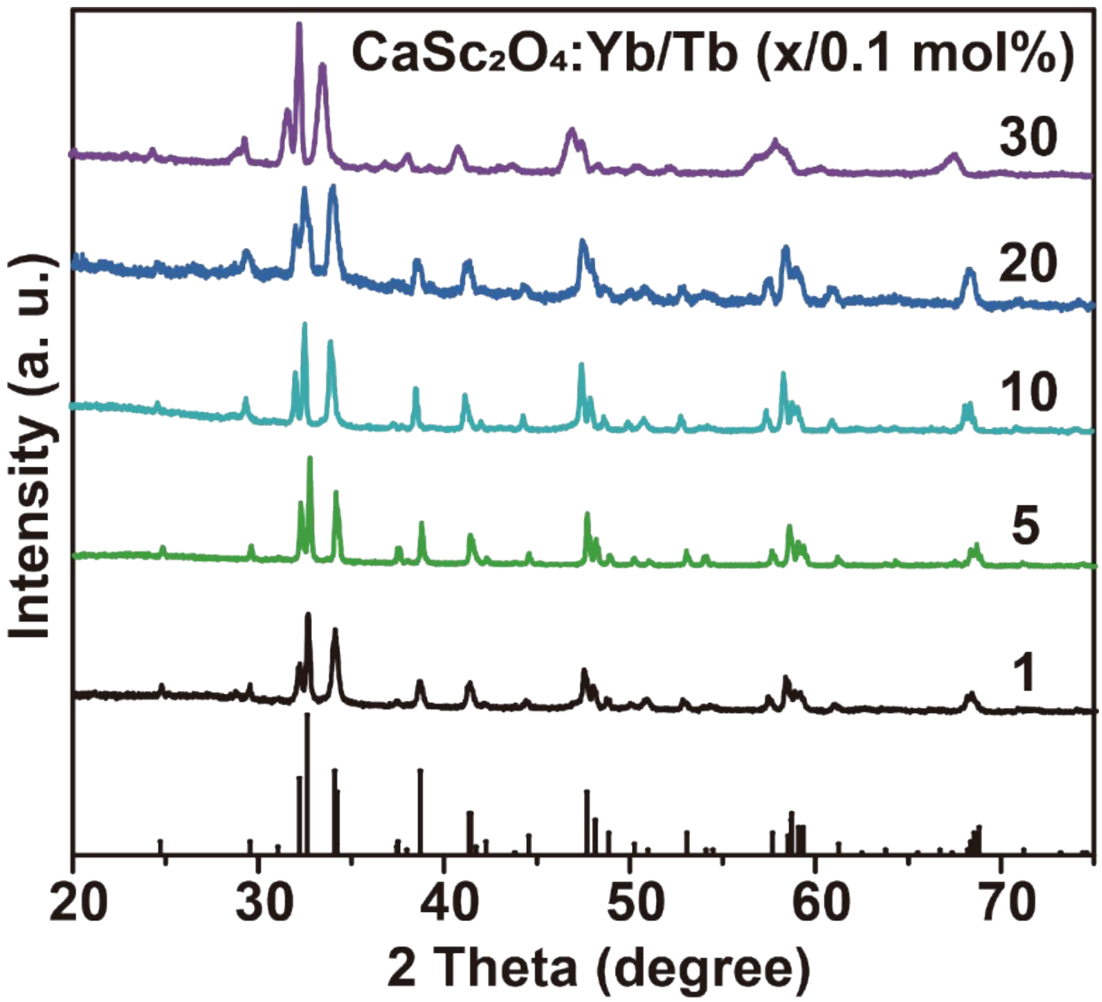

Fig. S1 XRD patterns of as-synthesized $CaSc_2O_4$:Yb/Tb (x/0.1 mol%, x = 1, 5, 10, 20, 30) powders. The diffraction pattern at the bottom is the literature reference of orthorhombic $CaSc_2O_4$ crystal (JCPDS: 20-0234).

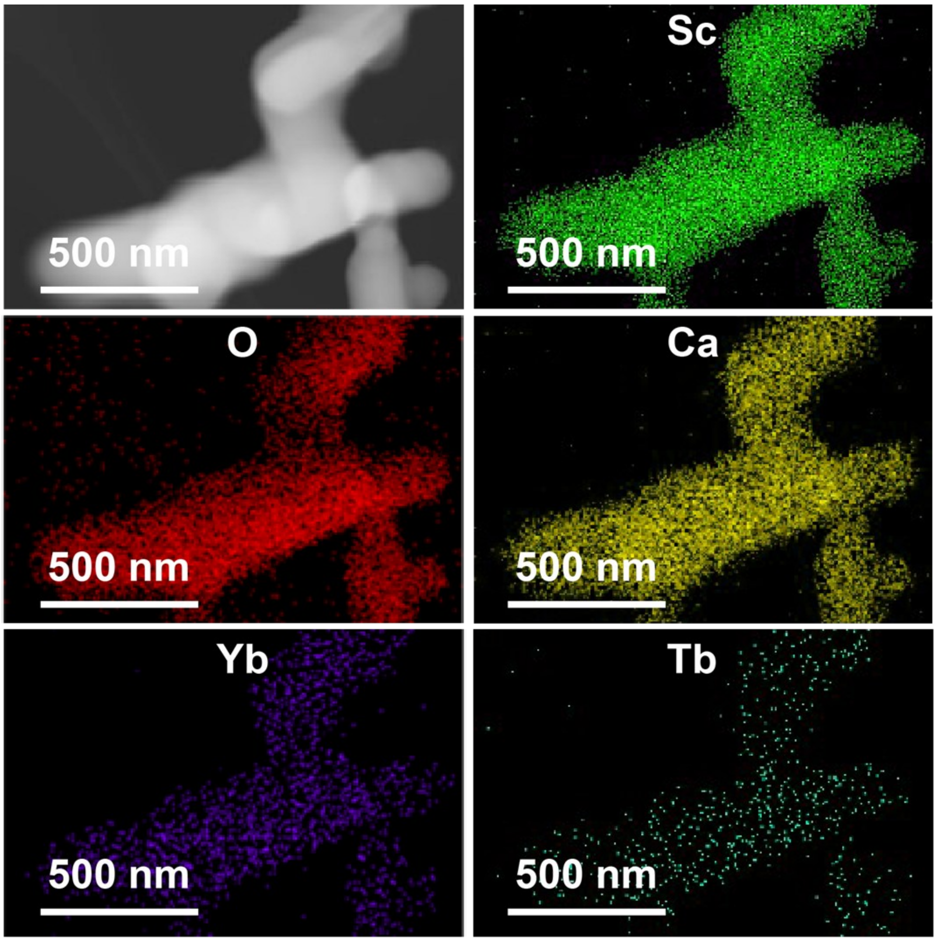

Fig. S2 EDX mapping results of $CaSc_2O_4$:Yb/Tb (5/0.1 mol%) powder.

Table S4 Elemental analysis of $CaSc_2O_4$: Yb/Ln (Ln = Tb^{3+} or Eu^{3+})

No.	Materials	Yb/Ln Doped (mol%)	Yb/Ln Detected (mol%)
1	$CaSc_2O_4$:Yb/Tb	Yb/Tb (5/0.1)	Yb/Tb (3.6/0.07)
2	$CaSc_2O_4$:Yb/Eu	Yb/Eu (5/2)	Yb/Eu (2.01/0.02)

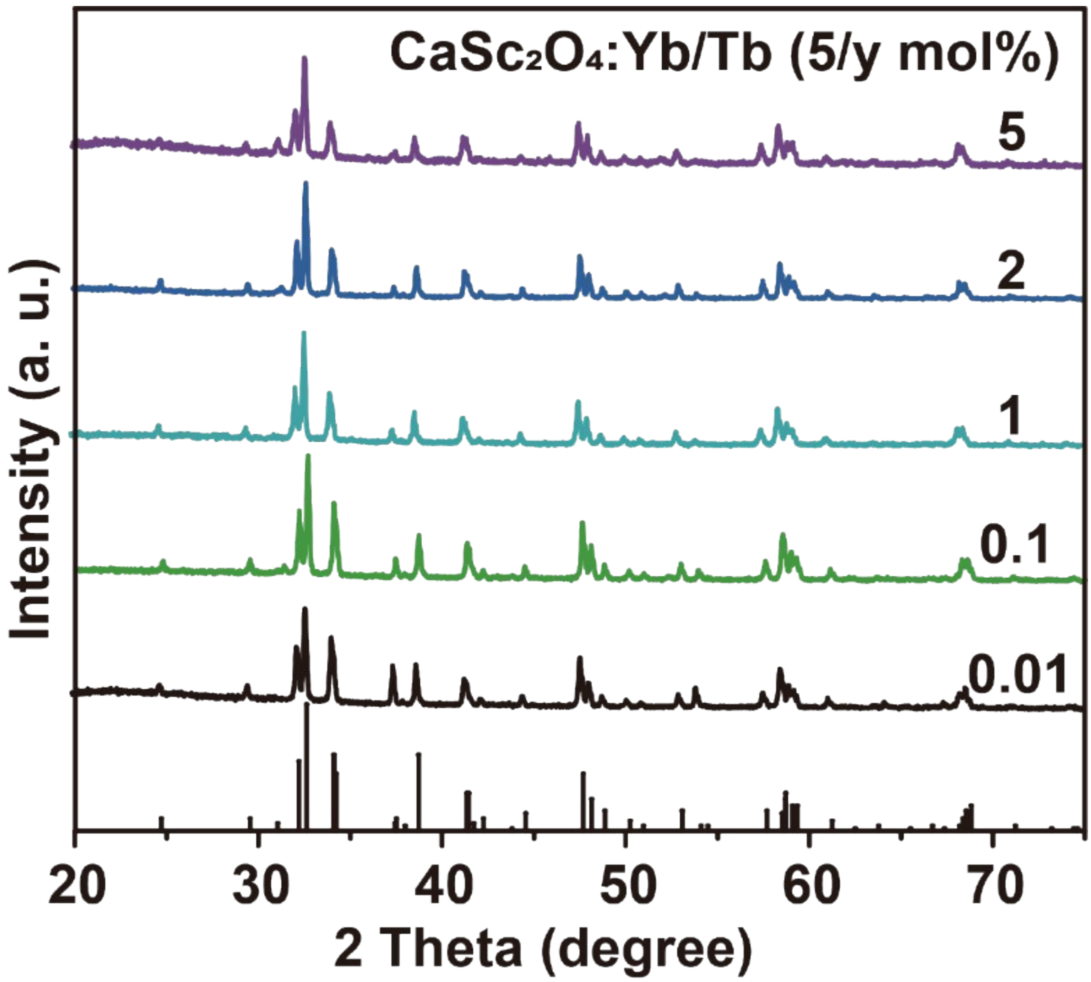

Fig. S3 XRD patterns of as-synthesized $CaSc_2O_4$:Yb/Tb (5/y mol%, y = 0.01, 0.1, 1, 2, 5) powders. The diffraction pattern at the bottom is the literature reference of orthorhombic $CaSc_2O_4$ crystal (JCPDS: 20-0234).

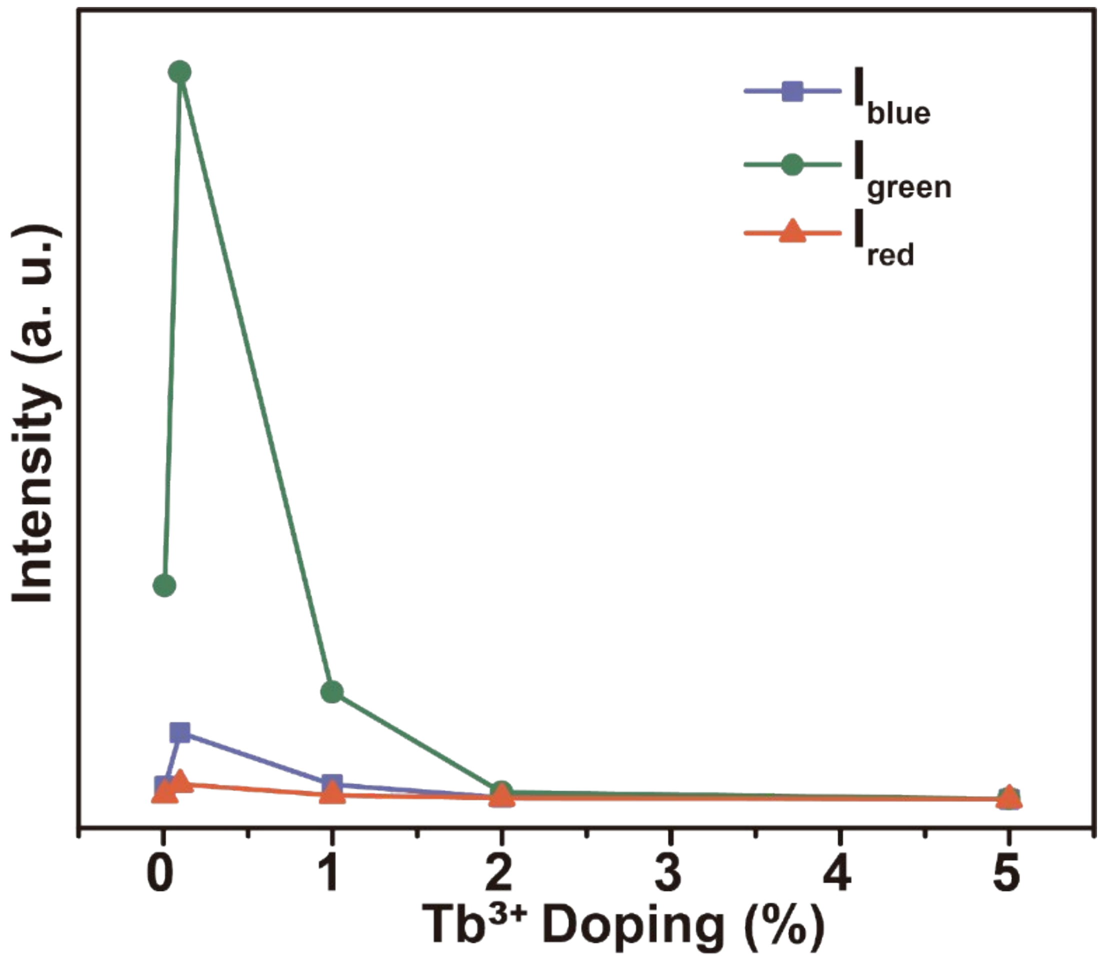

Fig. S4 The dependence of UCL emission intensity on Tb^{3+} doping concentration in $CaSc_2O_4$:Yb/Tb (5/y mol%, y = 0.01, 0.1, 1, 2, 5).

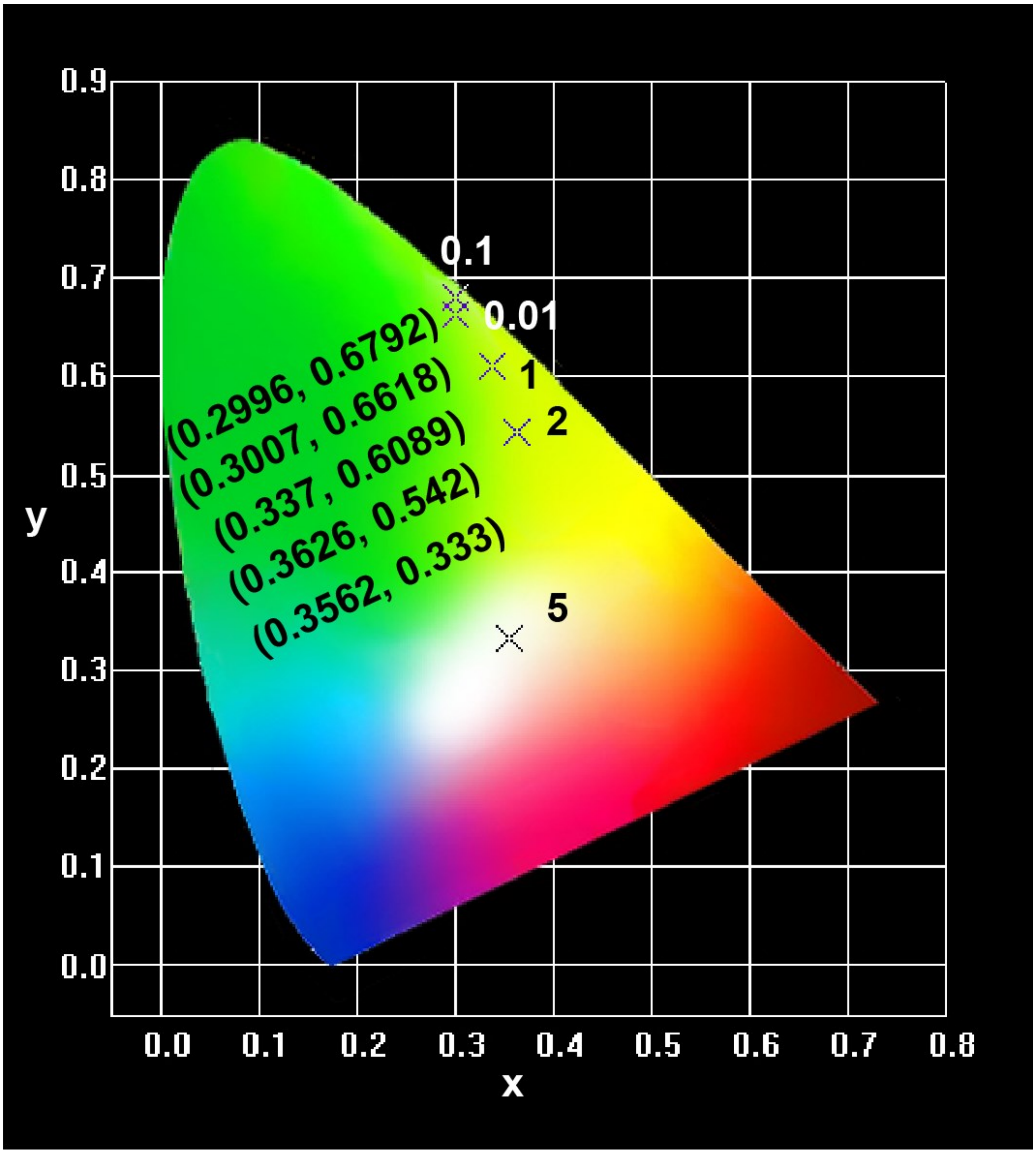

Fig. S5 The CIE color coordinates of $CaSc_2O_4$:Yb/Tb (5/y mol%, y = 0.01, 0.1, 1, 2, 5) powders.

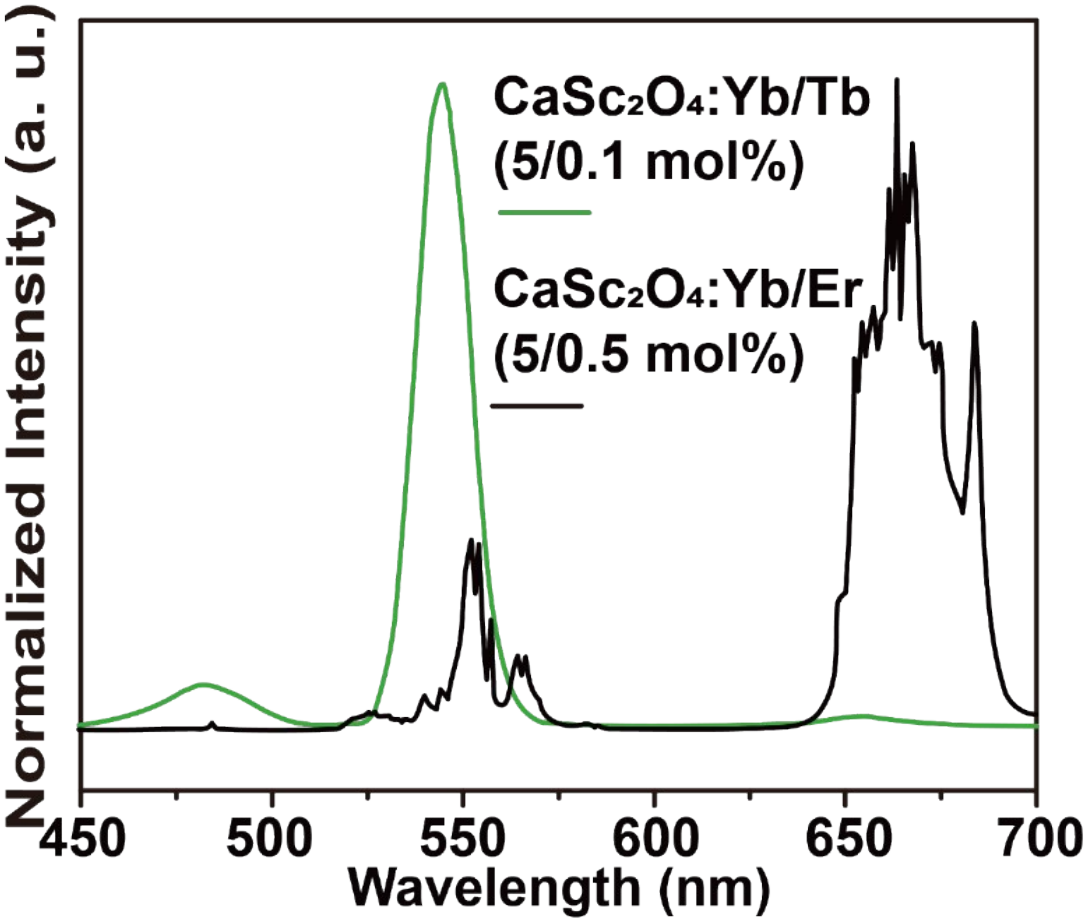

Fig. S6 Normalized intensity of UCL spectra of $CaSc_2O_4$:Yb/Tb (5/0.1 mol%) and $CaSc_2O_4$:Yb/Er (5/0.5 mol%) powders under the excitation of a 980 nm laser.

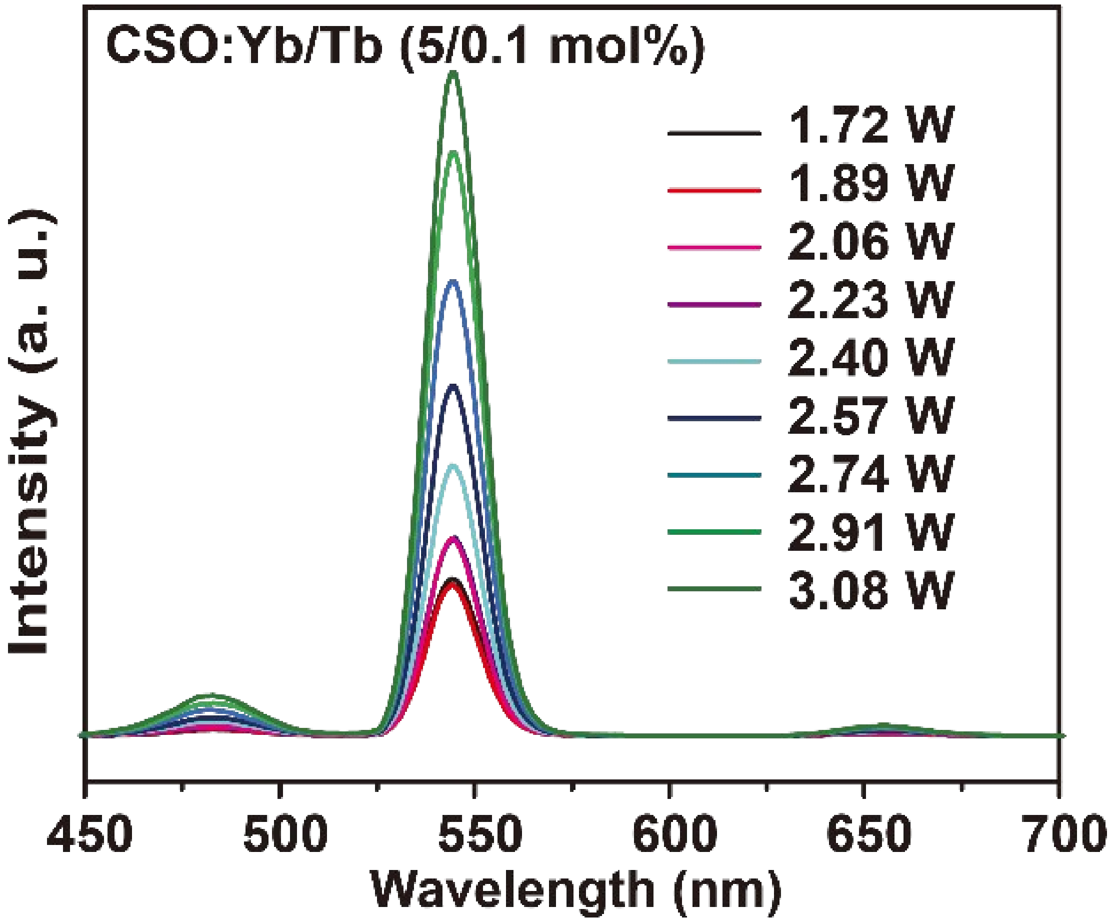

Fig. S7 UCL spectra of $CaSc_2O_4$:Yb/Tb (5/0.1 mol%) powders at different excitation powers of a 980 nm laser.

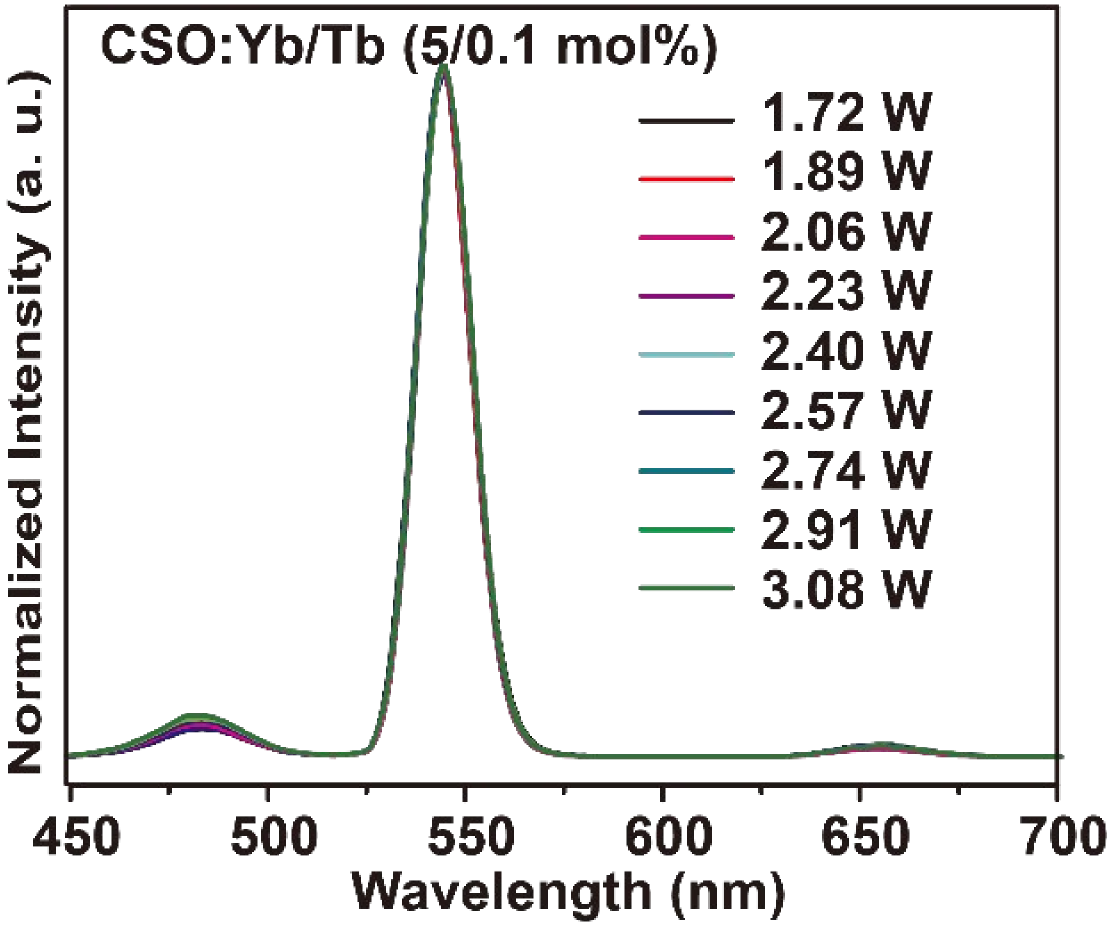

Fig. S8 Normalized intensity of UCL spectra of $CaSc_2O_4$:Yb/Tb (5/0.1 mol%) powders at different excitation powers of a 980 nm laser.

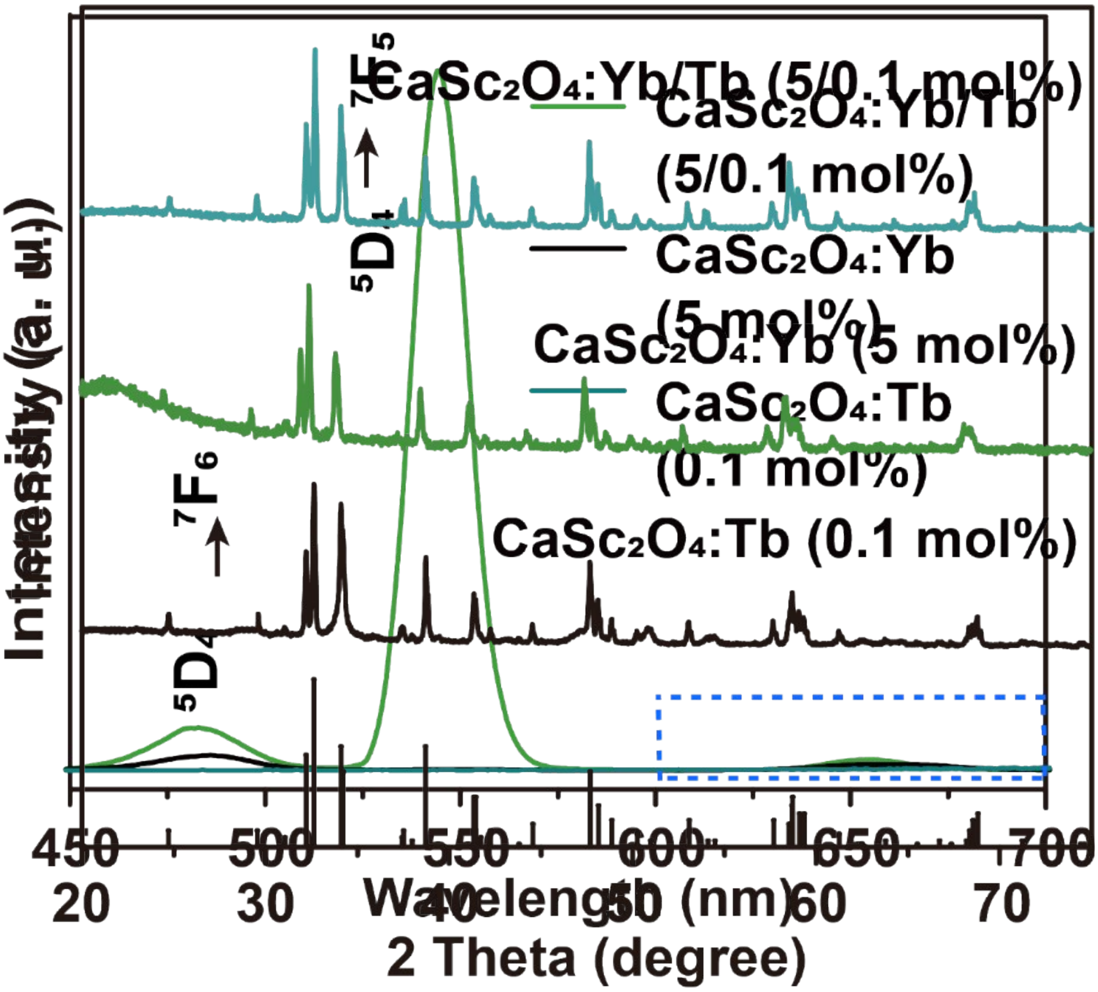

Fig. S9 XRD patterns of the as-synthesized $CaSc_2O_4$:Yb/Tb (5/0.1 mol%), $CaSc_2O_4$:Yb (5 mol%), and $CaSc_2O_4$:Tb (0.1 mol%) powders. The diffraction pattern at the bottom is the reference of orthorhombic $CaSc_2O_4$ crystal (JCPDS: 20-0234).

Fig. S10 UCL spectra of $CaSc_2O_4$:Yb/Tb (5/0.1 mol%), $CaSc_2O_4$:Yb (5 mol%) and $CaSc_2O_4$:Tb (0.1 mol%) powders under the excitation of a 980 nm laser.

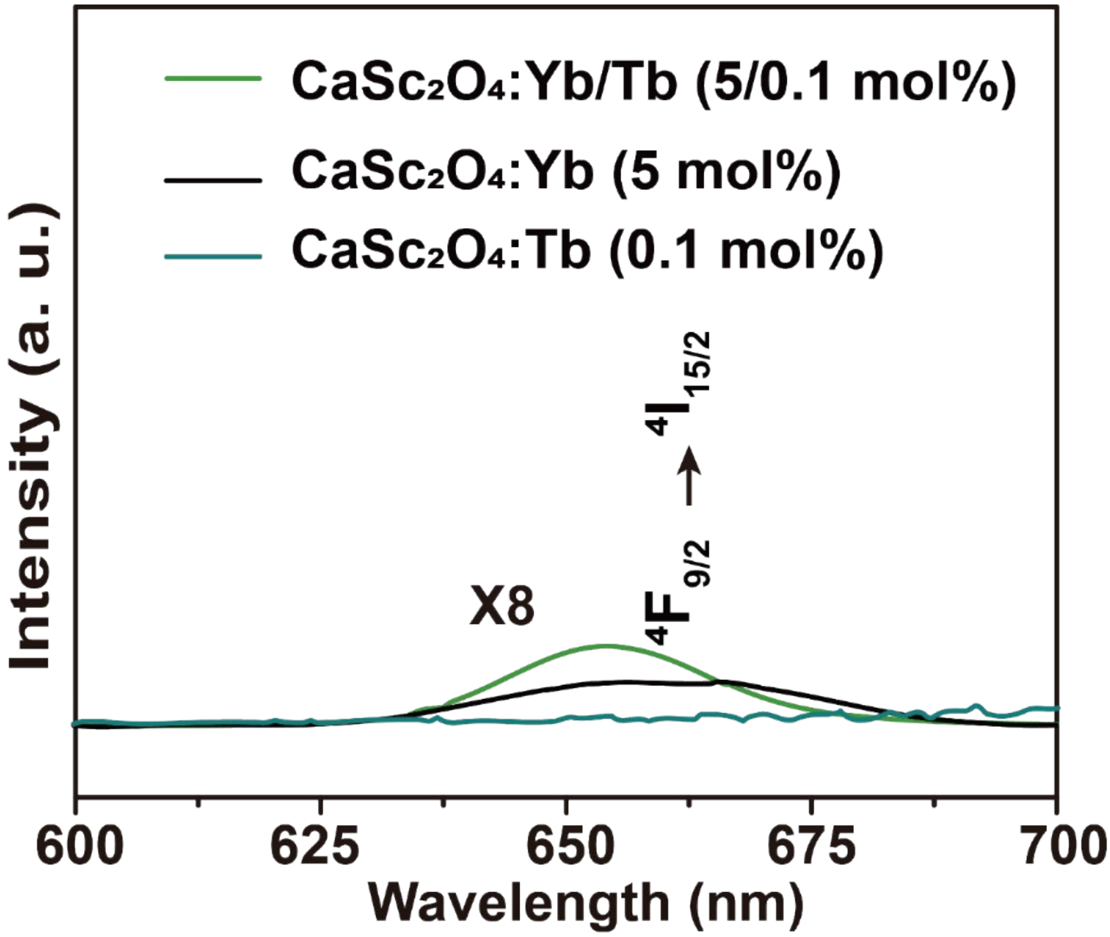

Fig. S11 The enlarged UCL spectra of $CaSc_2O_4$:Yb/Tb (5/0.1 mol%), $CaSc_2O_4$:Yb (5 mol%) and $CaSc_2O_4$:Tb (0.1 mol%) powders in the region of 600-700 nm under the excitation of a 980 nm laser.

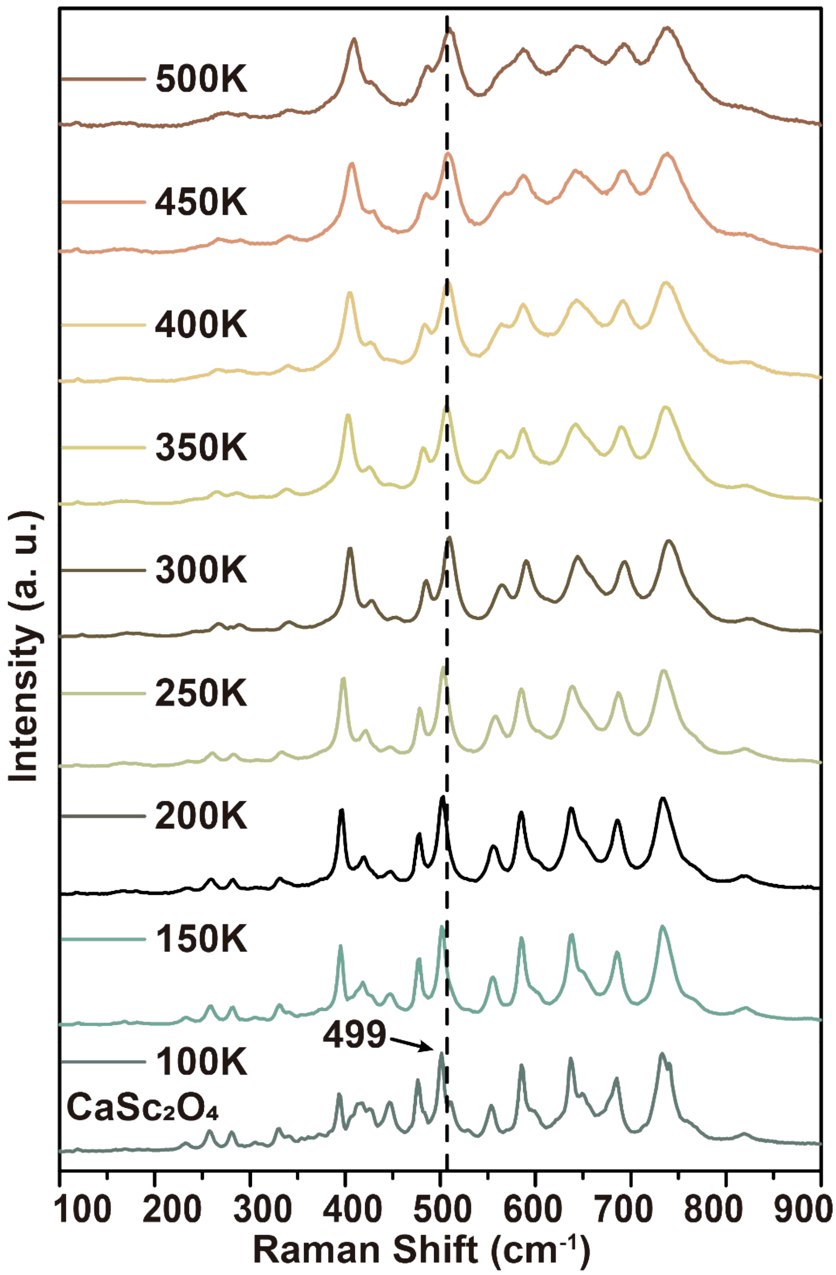

Fig. S12 Temperature-dependent Raman spectra of $CaSc_2O_4$ at temperature range of 100-500 K.

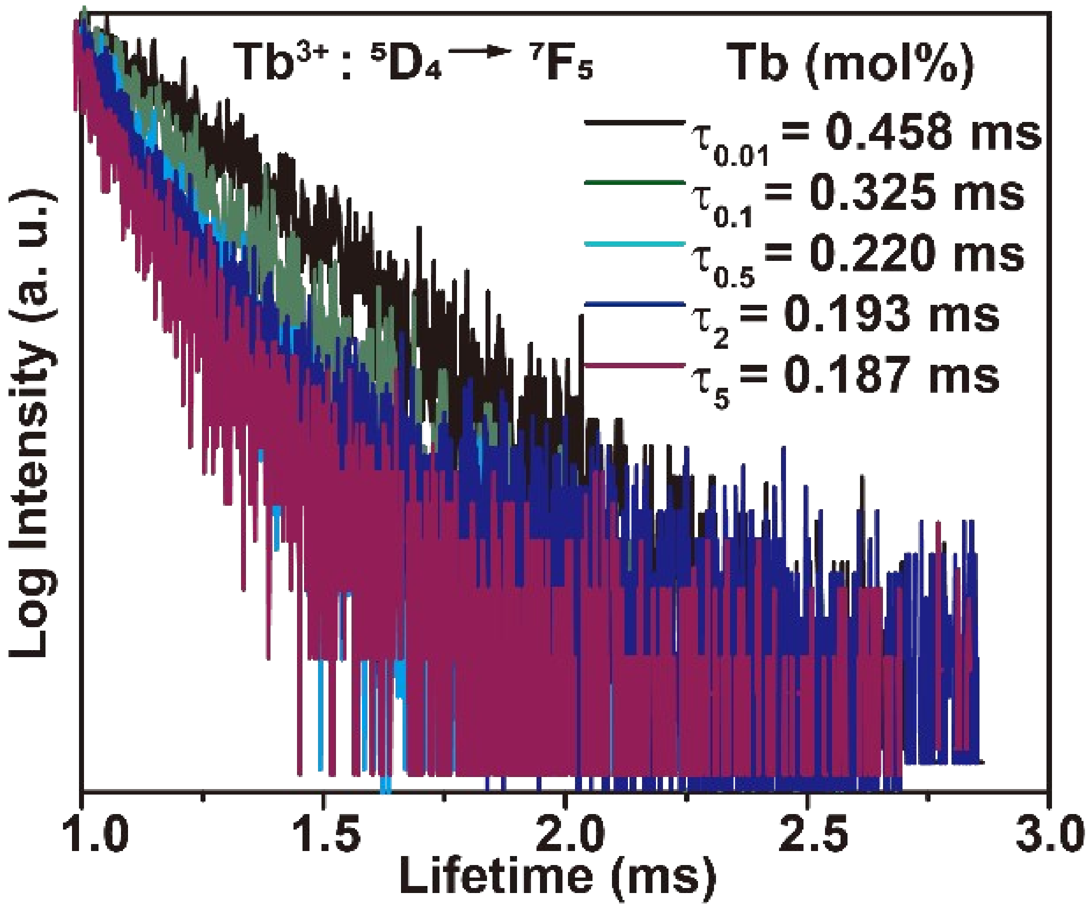

Fig. S13 UCL decay curves of $^5D_4 \rightarrow {}^7F_5$ transition of Tb^{3+} in $CaSc_2O_4$:Yb/Tb (5/y mol%, y = 0.01, 0.1, 1, 2, 5) powders excited under a 980 nm pulsed laser.

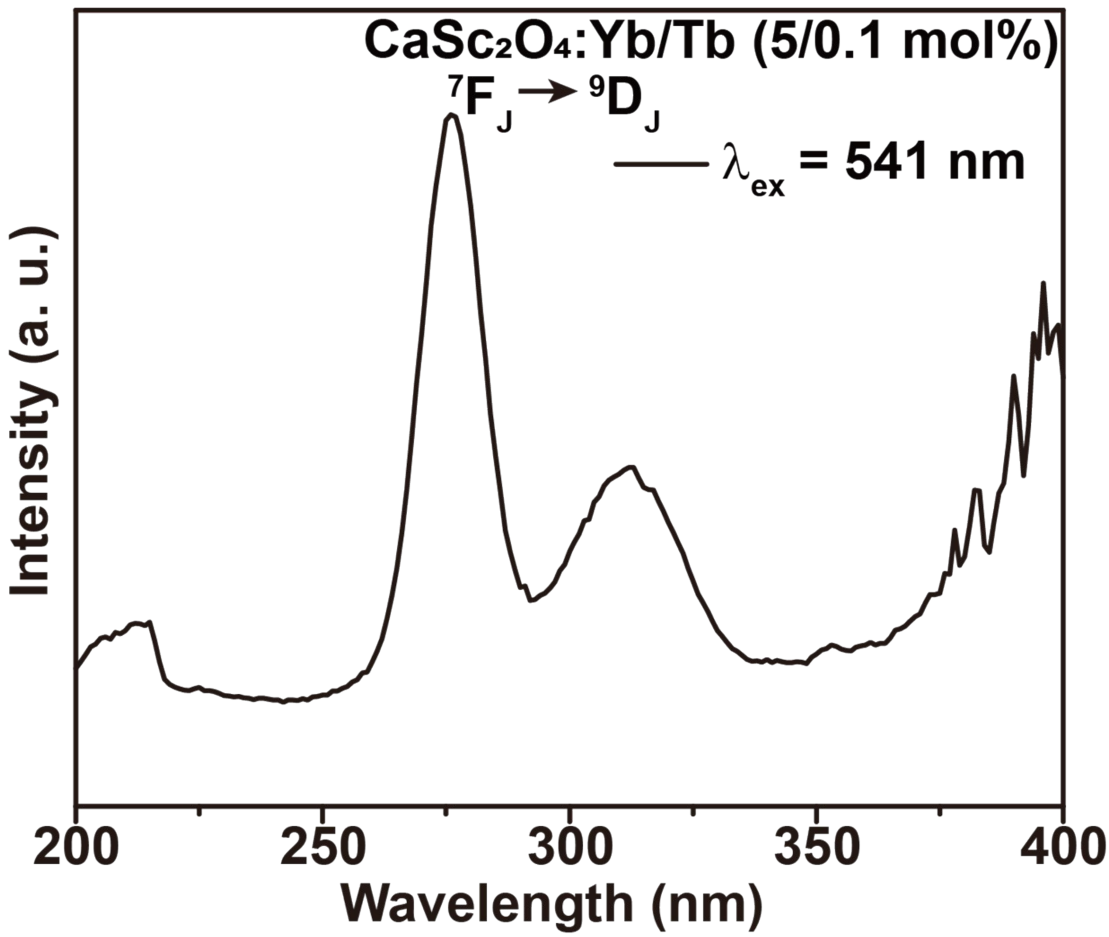

Fig. S14 Photoluminescence excitation spectrum of $CaSc_2O_4$:Yb/Tb (5/0.1 mol%) monitored at emission of 541 nm.

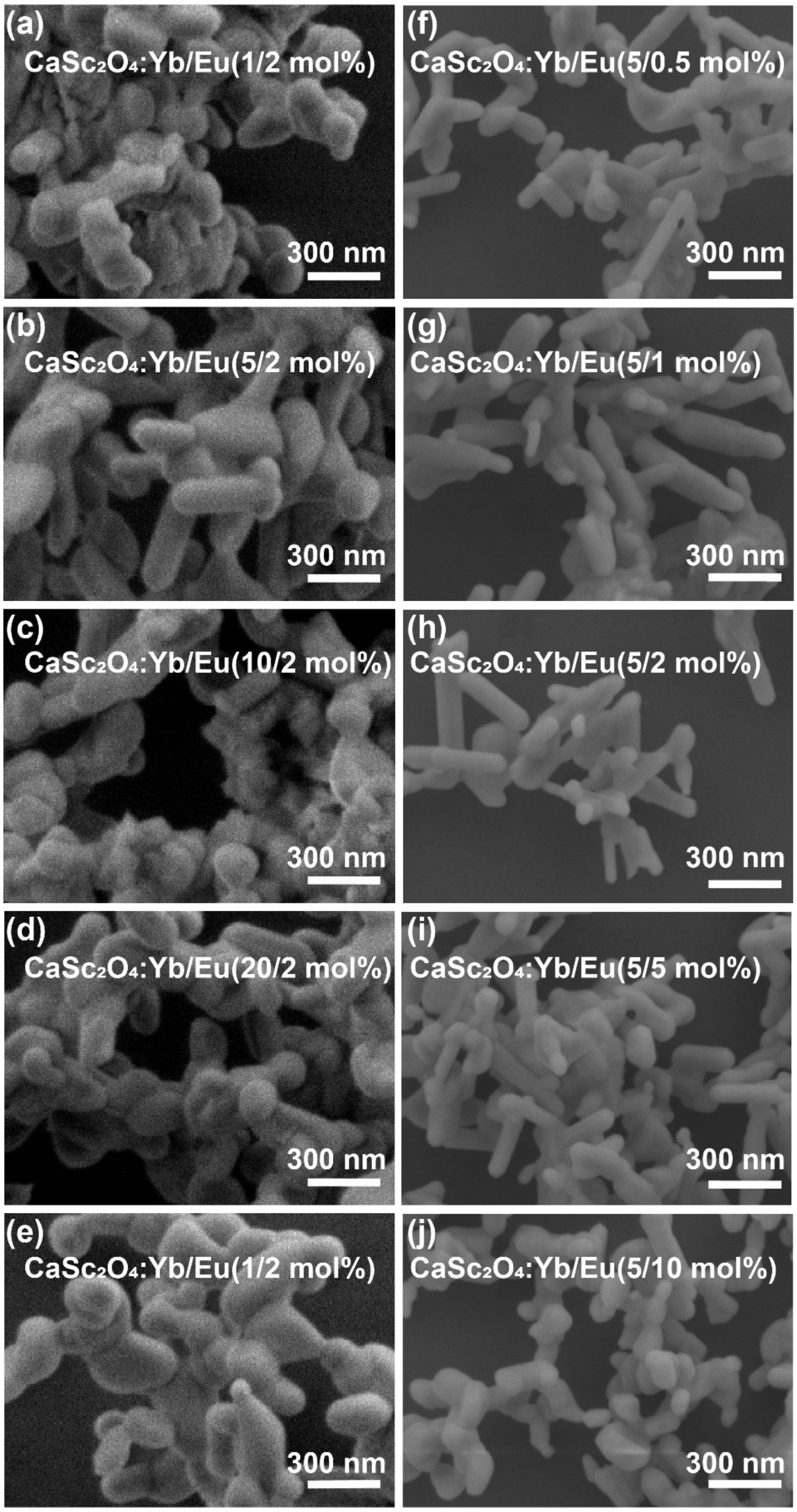

Fig. S15 SEM images of (a-e) as-synthesized $CaSc_2O_4$:Yb/Eu (x/2 mol%, x = 1, 5, 10, 20, 30) powders, (f-j) $CaSc_2O_4$: Yb/Eu (5/y mol%, y = 0.5, 1, 2, 5, 10) powders.

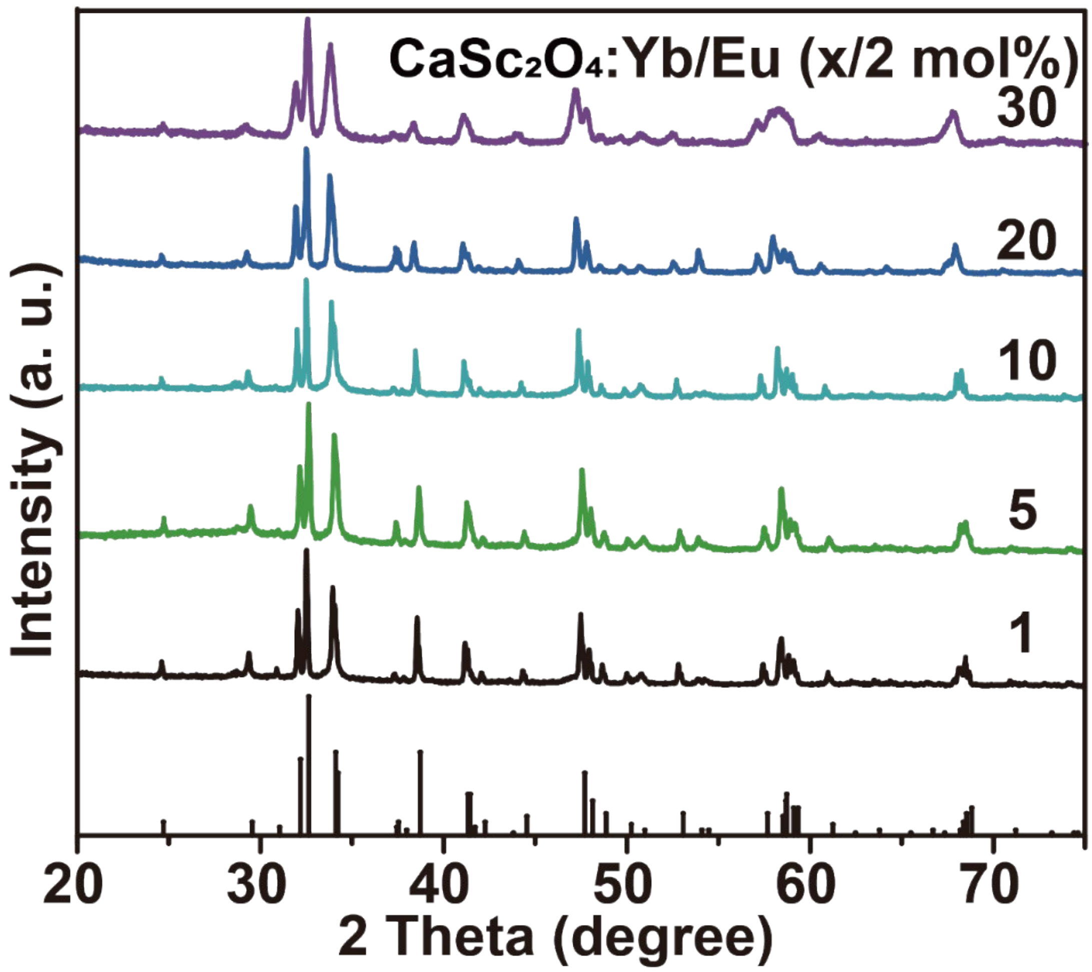

Fig. S16 XRD patterns of as-synthesized $CaSc_2O_4$:Yb/Eu (x/2 mol%, x = 1, 5, 10, 20, 30) powders. The diffraction pattern at the bottom is the literature reference of orthorhombic $CaSc_2O_4$ crystal (JCPDS: 20-0234).

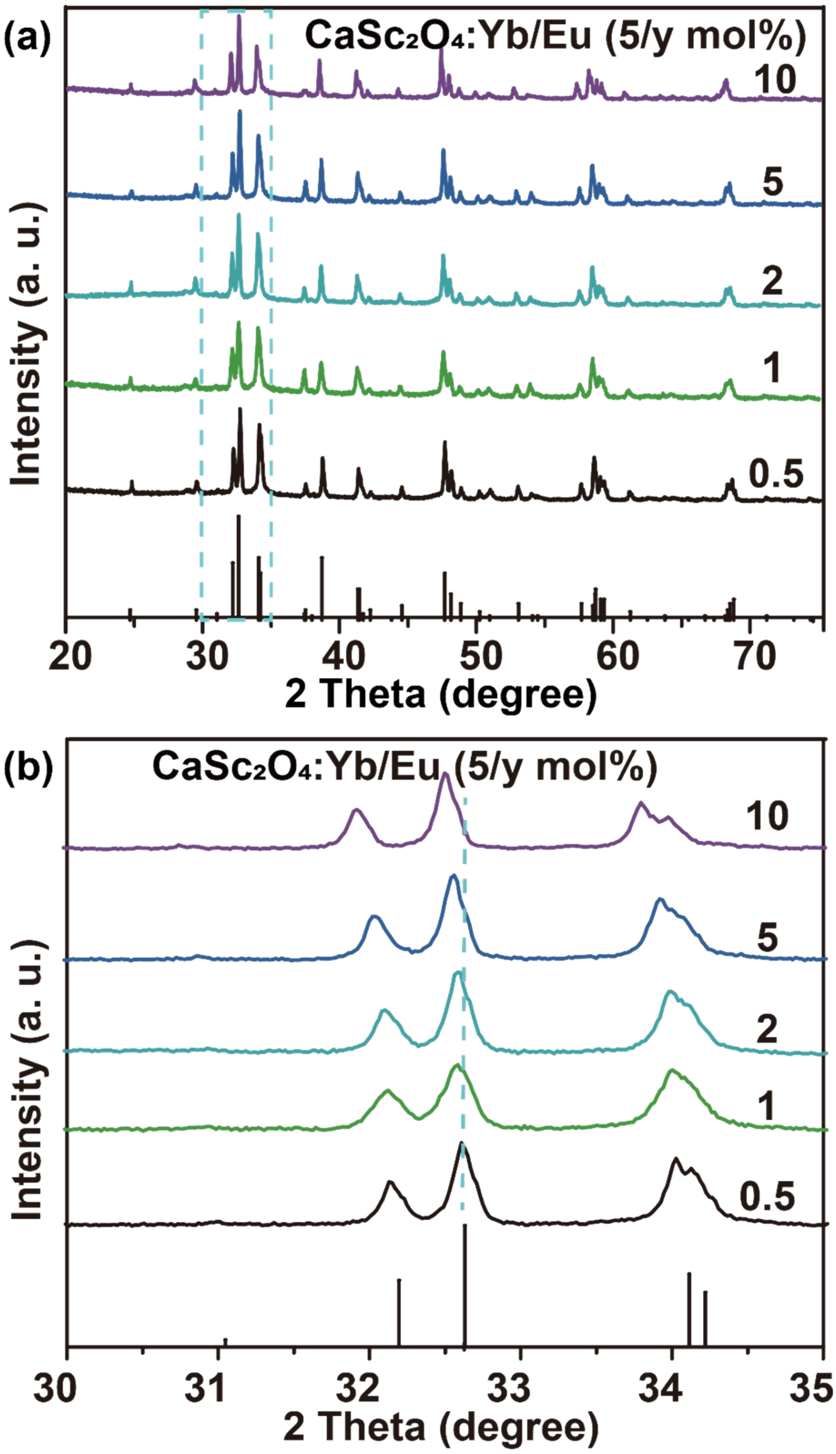

Fig. S17 (a) XRD and (b) enlarged XRD patterns of $CaSc_2O_4$:Yb/Eu (5/y mol%, y = 0.5, 1, 2, 5, 10) powders. The diffraction pattern at the bottom is the literature reference of orthorhombic $CaSc_2O_4$ crystal (JCPDS: 20-0234).

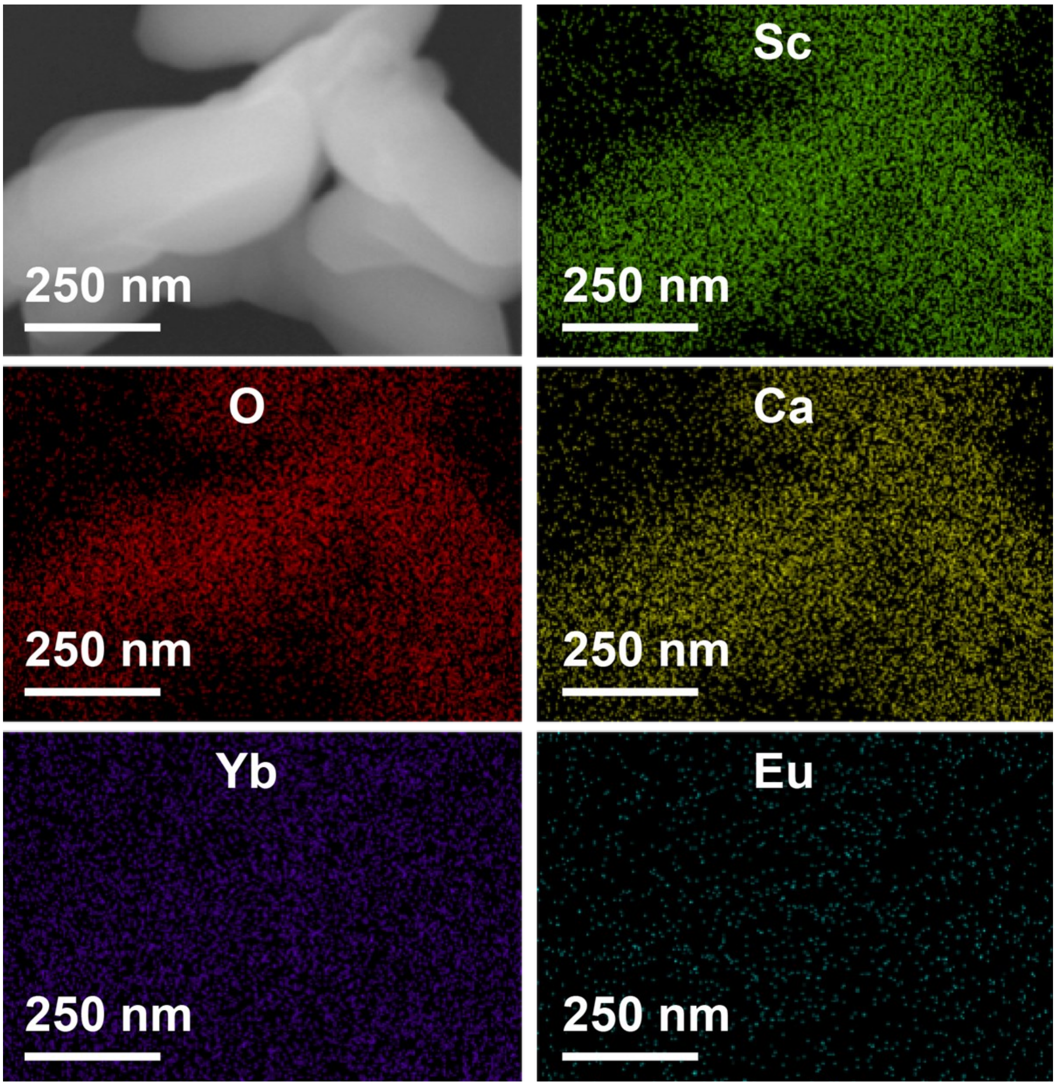

Fig. S18 EDX mapping results of $CaSc_2O_4$:Yb/Eu (5/2 mol%) powder.

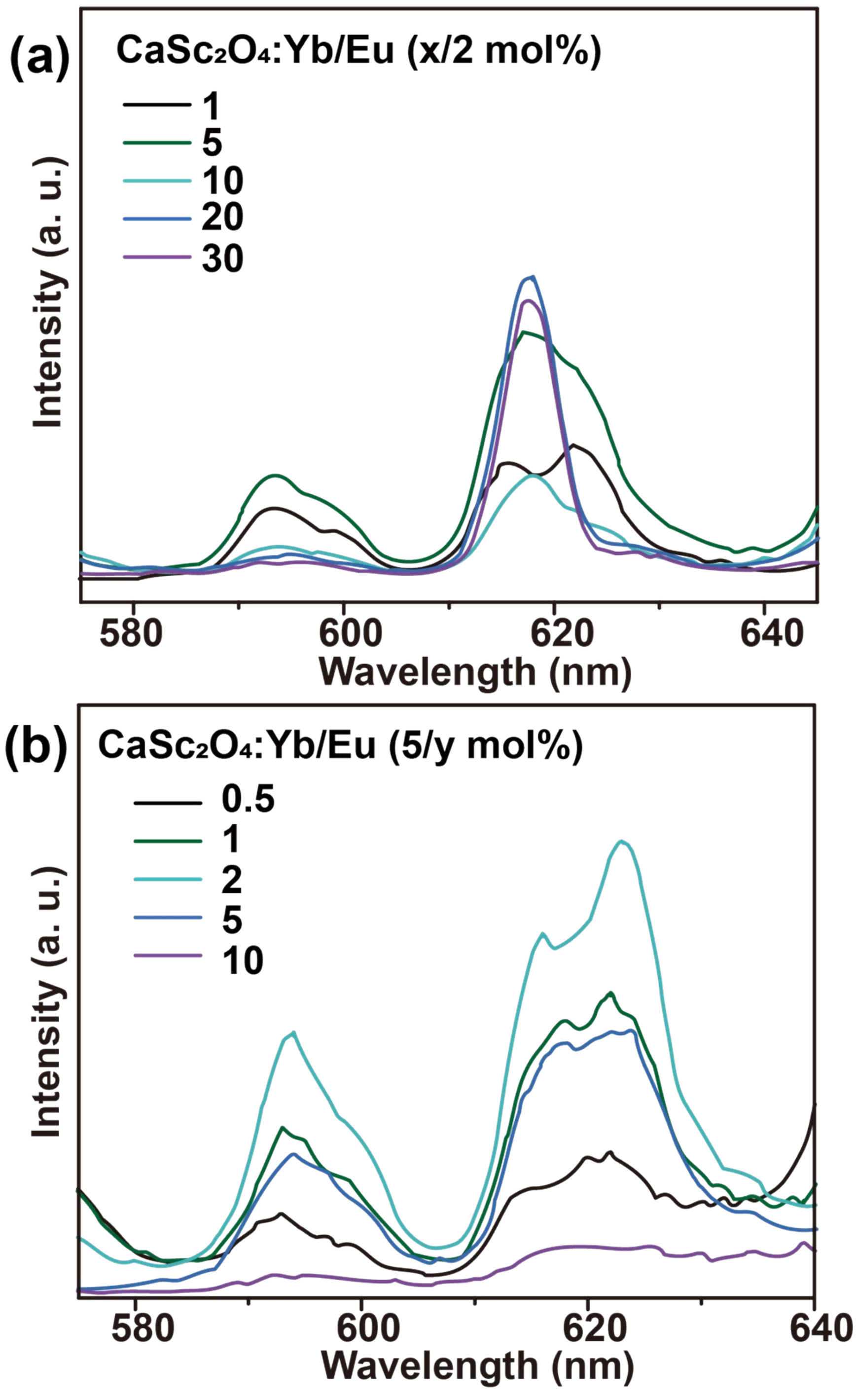

Fig. S19 (a) UCL spectra of $CaSc_2O_4$:Yb/Eu (x/2 mol%, x = 1, 5, 10, 20, 30) powders and (b) $CaSc_2O_4$:Yb/Eu (5/y mol%, y = 0.5, 1, 2, 5, 10) powders under the excitation of a 980 nm laser.

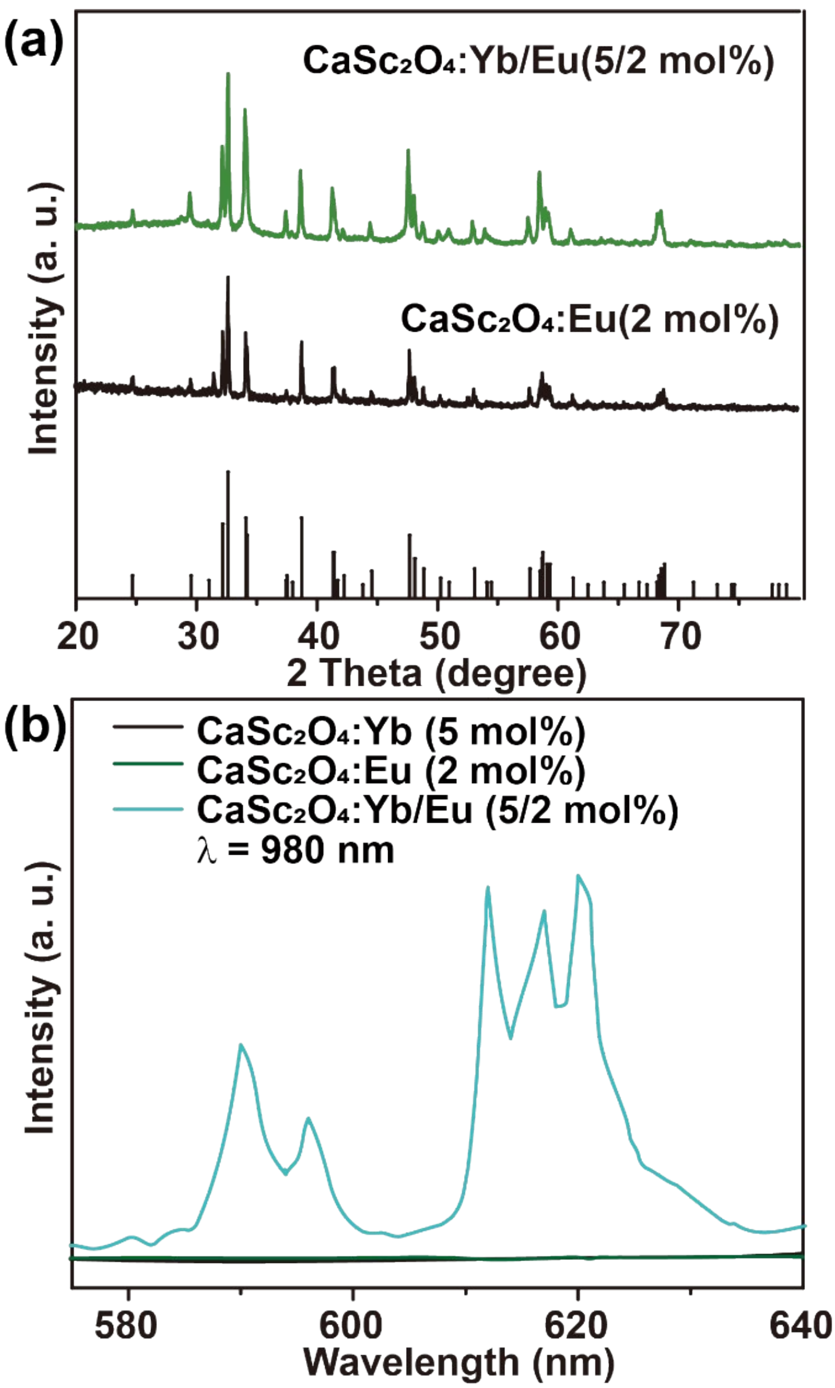

Fig. S20 (a) XRD patterns of as-synthesized $CaSc_2O_4$:Yb/Eu (5/2 mol%) and $CaSc_2O_4$:Eu (2 mol%) powders. The diffraction pattern at the bottom is the literature reference of orthorhombic $CaSc_2O_4$ crystal (JCPDS: 20-0234). (b) UCL spectra of $CaSc_2O_4$:Yb (5 mol%), $CaSc_2O_4$:Eu (2 mol%), and $CaSc_2O_4$:Yb/Eu (5/2 mol%) powders under the excitation of a 980 nm laser.

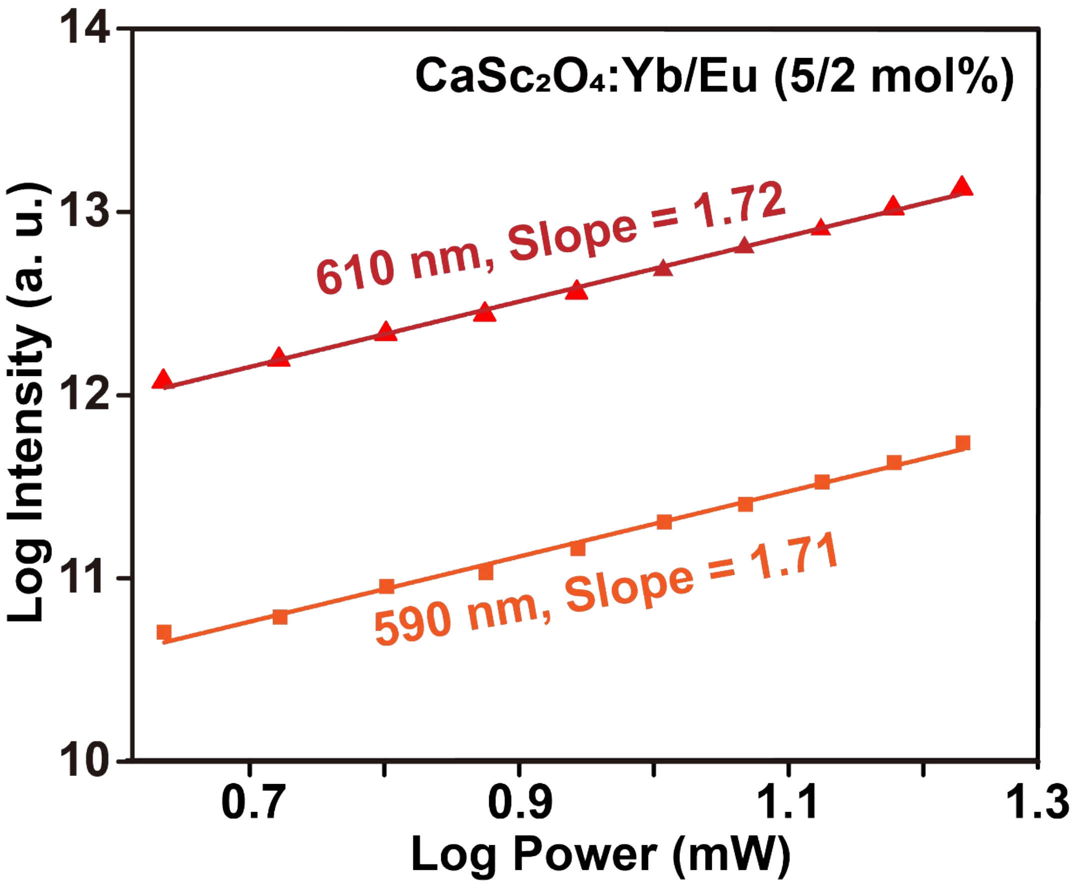

Fig. S21 Log-log plots of the upconversion emission intensities at 590 and 610 nm of $CaSc_2O_4$:Yb/Eu (5/2 mol%) powders versus excitation power of the 980 nm laser.

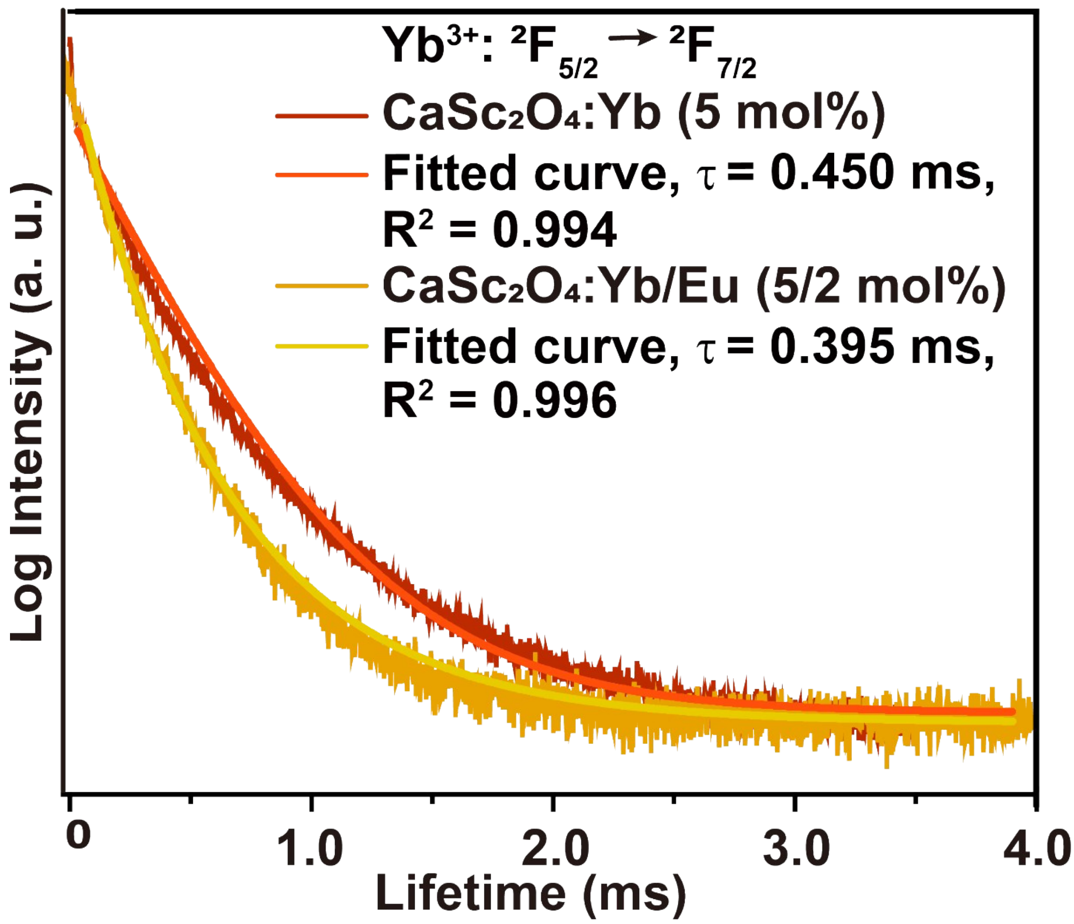

Fig. S22 Luminescence decay curves of $^2F_{5/2} \rightarrow {}^2F_{7/2}$ transition of Yb^{3+} in $CaSc_2O_4$:Yb (5 mol%) and $CaSc_2O_4$:Yb/Eu (5/2 mol%) powders, respectively, excited under a 980 nm pulsed laser.

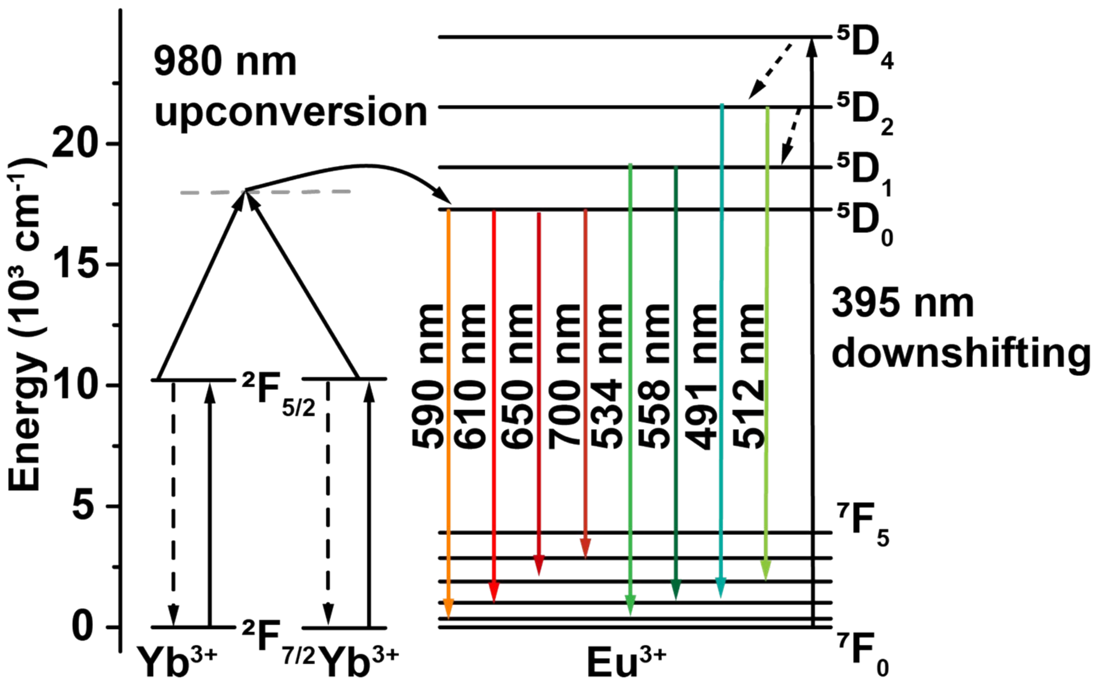

Fig. S23 Schematic illustration of the upconversion and downshifting luminescence mechanism in $CaSc_2O_4$:Yb/Eu under excitation of a 980 and 395 nm light, respectively.

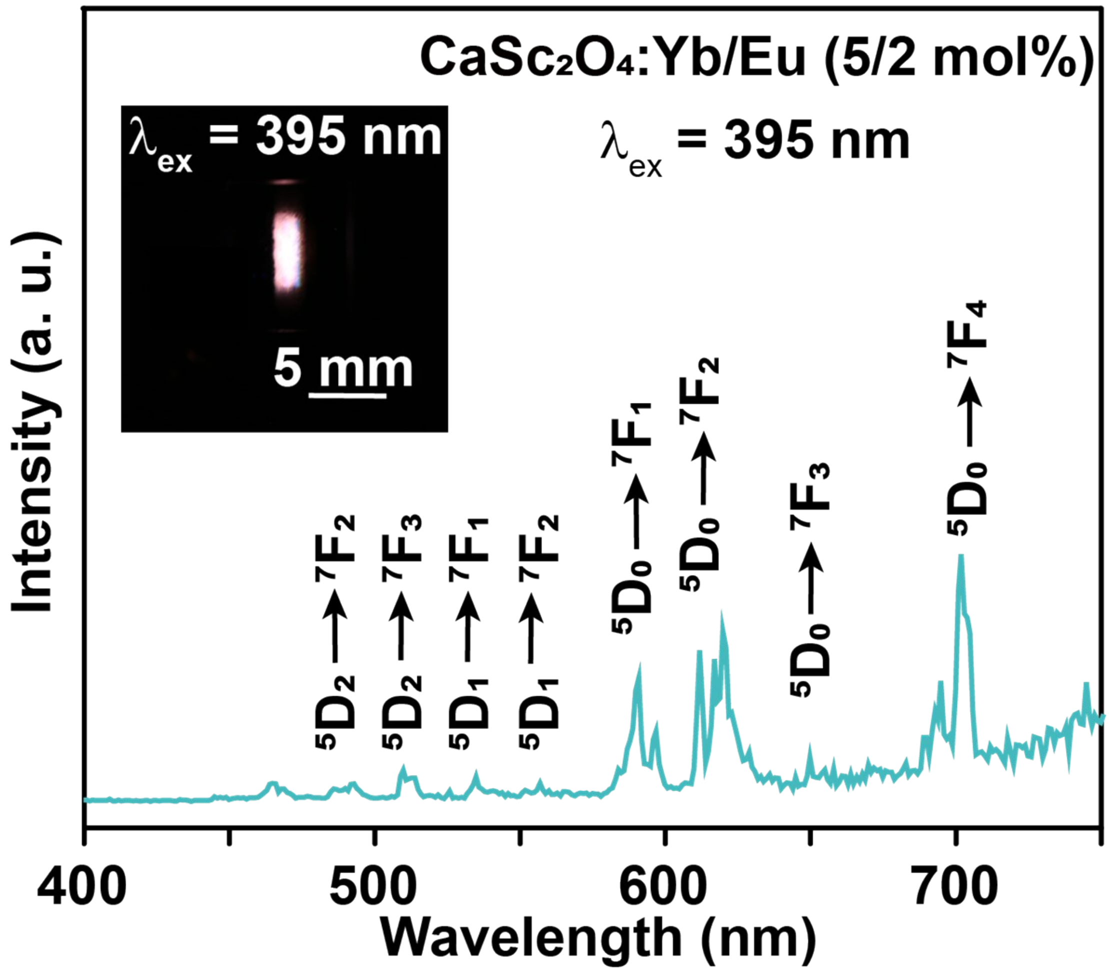

Fig. S24 Downshifting luminescence spectrum of $CaSc_2O_4$:Yb/Eu (5/2 mol%) excited by a 395 nm light. The inset is the photograph of $CaSc_2O_4$:Yb/Eu (5/2 mol%) powders under the excitation of a 395 nm.